A Residue Number System Based Parallel Communication Scheme Using Orthogonal Signaling: Part II—Multipath Fading Channels

Lie-Liang Yang, *Senior Member, IEEE,* and Lajos Hanzo, *Senior Member, IEEE*

***Abstract*—A novel signaling scheme is presented, where a set of orthogonal signals is transmitted in parallel. The signals are selected according to the so-called residue number system (RNS). Hence the system is essentially a multiple code parallel communication scheme using high-modulation alphabets. It is demonstrated that the system performance can be substantially improved by exploiting a number of advantageous properties of the RNS arithmetic.**

The model treated in Part I of this paper is extended here to account for the effects of the multipath Rayleigh fading channel when using noncoherent demodulation. Diversity reception techniques with equal gain combining (EGC) or selection combining (SC) are concerned. The related performance is evaluated for both nonredundant and redundant RNS-based orthogonal signaling. Interleaving and forward error-correction techniques are introduced for enhancing the system's bit error rate (BER) performance. The concept of concatenated coding with a Reed–Solomon (RS) code as the outer code and a redundant RNS code as the inner code is presented, and the performance of the proposed concatenated code is evaluated. Expressions of the error probability for the above-mentioned scenarios are presented, and the associated BER performance is evaluated numerically with respect to specific system parameters. Without concatenated coding, coding gains up to 8.5 or 11 dB are achieved at a BER of 10^{-6} using the lowest reliability dropping technique of Part I and one or two redundant moduli, respectively. The BER is substantially higher than that over the additive white Gaussian noise channel reported in Part I. With the aid of RS coding, an additional 7.5-dB coding gain is achieved.

***Index Terms*—Code-division multiple access (CDMA), concatenated coding, forward error correction, joint demodulation/decoding, M-ary orthogonal signaling, redundant residue number system (RRNS), residue number system (RNS).**

I. Introduction

In Part II of this paper, the analytical results obtained in Part I [4] will be extended to account for the effects of the multipath fading channel. The transmitted signal is impaired by the channel. In our receiver, several replicas of it can be obtained using diversity techniques, such as space diversity, time diversity, or frequency diversity.

Orthogonal signaling is well suited for noncoherent reception, and M-ary orthogonal signaling schemes with noncoherent demodulation have been used for practical systems [1]. For the noncoherent demodulation of M-ary orthogonal signaling schemes, equal gain combining (EGC) has been commonly used, whereby several multipath components are demodulated, equally weighted, and then added noncoherently. This technique is considered the optimal combining technique for noncoherent demodulation. However, from an implementational point of view, having a receiver complexity dependent on the number of resolvable paths is undesirable. Alternatively, a simple suboptimal selection combining (SC) scheme can be invoked [2], in which several multipath components are demodulated. The one having the highest amplitude (or signal-to-noise ratio) is selected for decision.

In this part of this paper, we focus our attention on the multipath fading channel, each path obeying a Rayleigh probability distribution. The bit error rate (BER) of the proposed residue number system (RNS)-based orthogonal signaling scheme for the above-mentioned two noncoherent diversity combining schemes—namely, for EGC and SC—is studied and the effects of the RNS arithmetic on the BER characterized. Furthermore, concatenated coding with a Reed–Solomon (RS) code as the outer code and a redundant RNS (RRNS) code as the inner code is proposed and its performance analyzed.

In the next section, the structure of the system is described and the channel and the receiver models are presented. Section III addresses the derivation of the BER without redundancy. In Section IV, the analytical results obtained for the additive white Gaussian noise (AWGN) channel are extended to the multipath Rayleigh fading channel. In Section V, the previously mentioned concatenated RS-RRNS coding is introduced for enhancing the system performance. Our numerical results and their interpretations are given in Section VI. Our summary and conclusions in Section VII complement this paper.

II. System Description

The functional block diagram shown in Fig. 1 illustrates the signal flow through a typical digital communication system including error-control coding, interleaving/deinterleaving, modulation, RNS processing, and the channel. The blocks of residue number system transform (RNST), inner encoder, orthogonal modulation, RNS processing, and inner decoder are similar to the related components described in Part I. The noncoherent demodulation block of Fig. 1 with EGC/SC for receiving the residue digit r_i is shown in Fig. 2, where the box of multipath diversity combining and maximum likelihood detection (MLD) includes the EGC or SC scheme and the detection. Finally, the output of the demodulation block U_i, as well as that of the ratio

Manuscript received November 17, 1999; revised November 19, 2001.

The authors are with the Department of Electronics and Computer Science, University of Southampton, SO17 1BJ Southampton, U.K. (e-mail: lly@ecs.soton.ac.uk; lh@ecs.soton.ac.uk).

Digital Object Identifier 10.1109/TVT.2002.804849

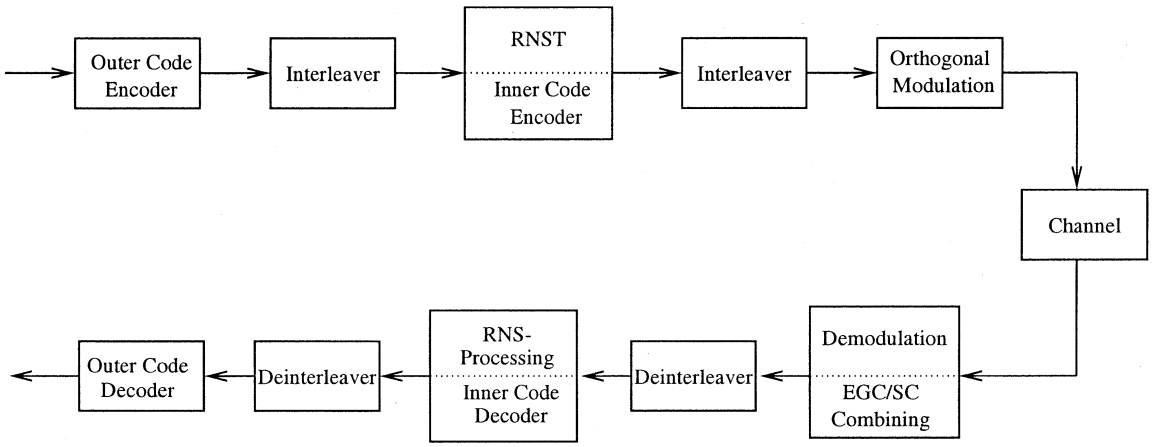

Fig. 1. Block diagram of the proposed system using error-control coding, orthogonal signaling, and RNS techniques.

statistic test (RST) λ_i, for $i = 1, 2, \ldots, u$, are input to the RNS-processing unit of Fig. 1. Error correction and interleaving are introduced, where in the various contexts error correction may be the outer error correction, the inner code correction, or the concatenated RS-RRNS code. The interleaving includes two stages: the outer interleaving and the inner interleaving. The interleaving here is used to randomize the burst errors induced by the fading of the channel and to enhance the efficiency of the error-control codes. The outer interleaving is an RS symbol interleaver, and the inner interleaving is a residue digit interleaver. The deinterleaved RS symbols and deinterleaved residue digits will be affected essentially independently by the channel impairments.

A. Channel Model

The low-pass equivalent impulse response of the multipath Rayleigh fading channel can be written as [3]

$$h(t) = \sum_{l=1}^{L_p} \beta_l e^{j\phi_l} \delta(t - \tau_l) \tag{1}$$

where $\delta(\cdot)$ is the Dirac function, while β_l, ϕ_l, and τ_l are, respectively, the lth path gain, phase shift, and time delay of the transmitted signal. The difference between the maximum and minimum values of τ_l is referred to as the maximum path delay spread, which is denoted by T_m. We assume that the maximum delay spread T_m is significantly less than the residue symbol duration T in order to avoid residue intersymbol interference. We assume that L_p number of transmitted signal replicas are available at the receiver. Each diversity path is assumed to be frequency-nonselective and slowly fading, while the fading processes on the L_p channels are assumed to be mutually statistically independent, exhibiting a uniform power-delay profile. Hence, for any input signal $s(t)$ expressed in the form of [4, (6)], the channel output signal $r(t)$ produced by the multipath fading channel consists of a sum of delayed, phase-shifted, and attenuated replicas of the input signal. Hence the low-pass equivalent received signal can be written as

$$r(t) = \sum_{l=1}^{L_p} \sum_{i=1}^{u} \beta_l e^{j\varphi_l} U_{ir_i}(t - \tau_l) + N(t) \tag{2}$$

where $\varphi_l = \phi_l - 2\pi f_c \tau_l$ is uniformly distributed in [0, 2π) and $N(t)$ represents a stationary zero-mean Gaussian random process with single-sided power spectral density of N_0.

B. Receiver Model

The receiver of Fig. 2 has a diversity structure; hence L number of multipath components will be tracked, where $L = 1$, 2, 3, ..., and the actual number of combined branches of $L \leq L_p$ depends on the maximum acceptable complexity of the receiver, although there are L_p number of transmitted signal replicas at the receiver. The received signal is first input to u banks of decorrelators for receiving the u transmitted residue digits, as seen in [4, Fig. 2]. Each bank of decorrelators processes one residue digit. For a residue digit with related modulus m_i and an Lth order diversity receiver, $m_i L$ decorrelators are required for receiving the residue digit r_i.

After correlation, the decision variables will be combined according to the investigated EGC or SC multipath diversity reception methods. Following the multipath diversity reception stage, the next step is RNS processing, which is similar to [4, Section II of Fig. 2]. Error-dropping-only decoding, error-correction-only decoding, and error-dropping-and-correction decoding can be introduced in order to optimize the system's performance. Finally, v number of RNS-processing outputs are mapped to the residue digits with respect to the related moduli and then input to the inverse RNST block of [4, Fig. 2] in order to transform the RNS based information to binary information. After the RS code symbols are received, the symbol errors might be corrected by the outer RS decoding.

III. Performance Without RNS Processing

In this section, we first compute the output variables of the square-law detectors [3] invoked for receiving the different residue digits over the lth diversity channel, where $l = 1, 2, \ldots, L \leq L_p$. Then the BER performance of the uncoded system without RNS processing is evaluated using EGC and SC.

Let the uncoded information symbol be $N = 0$, which is represented by a residue sequence of {0, 0, ..., 0} with respect to

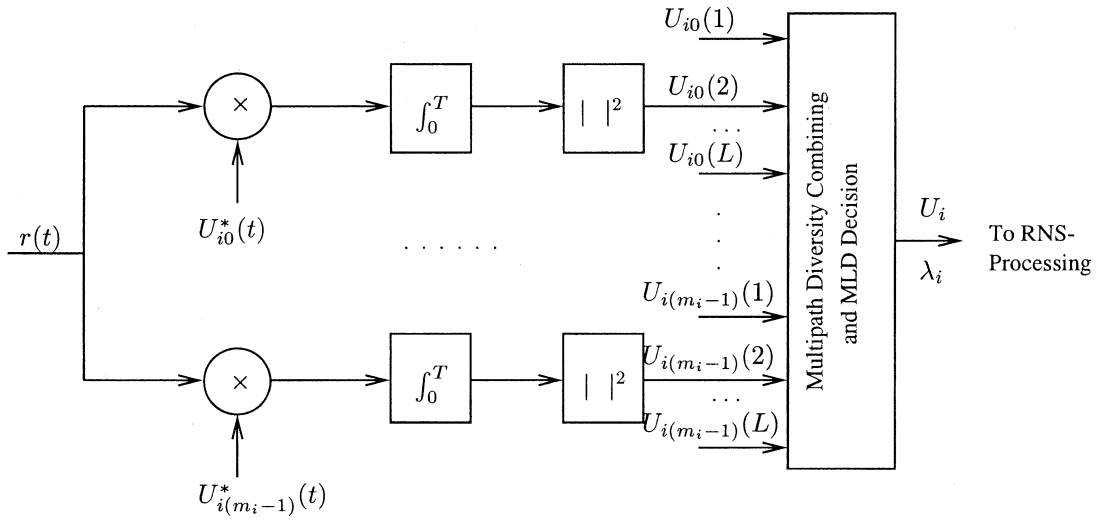

Fig. 2. The noncoherent demodulation branch for receiving residue digit r_i.

moduli $\{m_1, m_2, \ldots, m_u\}$. Since no RNS processing is considered in this section, i.e., no redundant RNS is used; hence $v = u$ and the information dynamic range becomes $M = \prod_{i=1}^{u} m_i$. Let U_{ij}^l, $i = 1, 2, \ldots, u$, $j = 0, 1, \ldots, m_i - 1$ be the output of the square-law detector assigned to the ith residue digit received over the lth diversity channel. Since the symbol $N = 0$ was assumed to be transmitted, U_{ij}^l can be expressed as [3]

$$U_{i0}^l = \left| \frac{2\xi}{u} \beta_l e^{j\varphi_l} + N_{i0} \right|^2, \ i = 1, 2, \ldots, u \tag{3}$$

$$U_{ij}^l = |N_{ij}|^2, \ i = 1, 2, \ldots, u; \ j = 1, 2, \ldots, m_i - 1 \tag{4}$$

when an equal transmitted energy is assumed for each of the u number of residue digits (this assumption is maintained throughout this part of the paper), where N_{ij} is a zero-mean complex Gaussian random variable with variance $4\xi N_0/u$ and the channel gain coefficient $\beta_l e^{j\varphi_l}$ is also a zero-mean complex Gaussian random variable with variance $E[\beta_l^2]$. Here, $E[\cdot]$ represents the expected value of the argument. Taking the expectation of (3) and (4), the mean of U_{i0}^l is $\overline{U}_{i0}^l = \left(4\xi^2 E[\beta_l^2]/u + 4\xi N_0\right)/u$ and the mean of each U_{ij}^l for $i = 1, 2, \ldots, u$ and $j \neq 0$ is $\overline{U}_{ij}^l = 4\xi N_0/u$. Let us now derive the expressions of the average error probabilities for the receiver using EGC and SC.

A. Equal Gain Combining

For a receiver with Lth order ($L \leq L_P$) diversity reception and EGC, the L branches are equally weighted and then added in order to form the decision variables, which can be expressed as

$$U_{ij} = \sum_{l=1}^{L} U_{ij}^l \tag{5}$$

for $i = 1, 2, \ldots, u$ and $j = 0, 1, \ldots, m_i - 1$.

Since the symbols are orthogonal and the additive noise processes are mutually statistically independent, the random variables $\{U_{ij}\}$ are also mutually statistically independent. The probability density functions (pdfs) of $\{U_{ij}\}$ are chi-square distributed [3] with $2L$ degree of freedom. After normalization by $\overline{U}_{ij}^l = 4\xi N_0/u$, the pdfs of $\{U_{ij}\}$ can be expressed upon modifying Proakis' approach [3, p. 828, (14.4–31) and (14.4–32)]

$$f_{U_{i0}}(x) = \frac{1}{(1+\overline{\gamma}_0)^L (L-1)!} x^{L-1} \exp\left(-\frac{x}{1+\overline{\gamma}_0}\right), \ x \geq 0 \tag{6}$$

$$f_{U_{ij}}(x) = \frac{1}{(L-1)!} x^{L-1} \exp(-x), \ x \geq 0 \tag{7}$$

for $i = 1, 2, \ldots, u$, where $\overline{\gamma}_0 = E\left[\beta_l^2\right] \xi/(uN_0) = E\left[\beta^2\right] \xi/(uN_0)$ and the index $j = 0$ corresponds to the pdfs $f_{U_{i0}}(x)$, $i = 1, 2, \ldots, u$, associated with the correlator outputs matched to the transmitted residue sequence of (0,0, …, 0), while $f_{U_{ij}}(x)$, $i = 1, 2, \ldots, u$, $j = 1, 2, \ldots, m_i - 1$, corresponds to the distributions of the correlator outputs mismatched to the transmitted residues' sequence. The probability that the residue digit r_i, $i = 1, 2, \ldots, u$ will be decoded correctly—remembering that $U_{i0}(t)$, $i = 1, 2, \ldots, u$, was transmitted—can be written as

$$P_i(C) = P\left(U_{i1} < U_{i0}, U_{i2} < U_{i0}, \ldots, U_{i(m_i-1)} < U_{i0}\right). \tag{8}$$

Assuming that U_{ij}, $j = 1, 2, \ldots, m_i - 1$, are independent identically distributed (i.i.d.) random variables, then (8) can be shown to lead to

$$P_i(C) = \int_0^\infty \frac{1}{(1+\overline{\gamma}_0)^L (L-1)!} y^{L-1} \exp\left(-\frac{y}{1+\overline{\gamma}_0}\right) \cdot \left[1 - \exp(-y) \sum_{k=0}^{L-1} \frac{y^k}{k!}\right]^{m_i - 1} dy. \tag{9}$$

Since no redundant moduli are considered in this section, a symbol is received correctly if and only if all residue digits are received correctly. Hence, the probability $P_s(C)$ of correct symbol recovery can be expressed as the product of receiving all

residue digits constituting the symbol correctly, which is given by

$$P_s(C) = \prod_{i=1}^{u} P_i(C). \tag{10}$$

Lastly, the BER $P_b(\epsilon)$ can be approximated as [3, p. 260, (5.2.24)]

$$P_b(\epsilon) \approx \frac{1}{2}(1 - P_s(C)) \tag{11}$$

when the number of bits per symbol is high.

B. Selection Combining

For an L-branch diversity receiver with SC—where the branch signal with the highest amplitude is selected for demodulation—the decision variables are given by (3) and (4) for the lth multipath component when the residue sequence (0, 0, ..., 0) is transmitted. These decision variables are exponentially distributed, and their pdfs can be expressed as [3, p. 44, (2.1–126)]

$$f_{U_{ij}^l}(x) = \lambda_{ij} e^{-\lambda_{ij} x},\ x \geq 0 \tag{12}$$

for $i = 1, 2, \ldots, u$ and $j = 0, 1, \ldots, m_i - 1$, where $\lambda_{i0} = u^2/\left(4\xi^2 E[\beta^2] + 4\xi N_0 u\right)$ when $j = 0$ or $\lambda_{ij} = u/(4\xi N_0)$ when $j \neq 0$ following the output of the decorrelators matched or mismatched to the transmitted residue digit r_i, respectively.

Since the branch signal having the highest amplitude is selected for demodulation, the residue digit r_i will be received correctly if there is no U_{ij}^l value for $j \neq 0$ and $1 \leq l \leq L$ that is larger than the maximum output of U_{i0}^l with $1 \leq l \leq L$, corresponding to the message N. Let us assign $U_{i0,\max} = \max\left\{U_{i0}^l \text{ for } l = 1, 2, \ldots, L\right\}$ and $U_{ij,\max} = \max\left\{U_{ij}^l \text{ for } l = 1, 2, \ldots, L \text{ and } j \neq 0\right\}$. Assuming that the average signal-to-noise ratio (SNR) on each diversity reception path is equal and the noise processes are i.i.d. variables, then upon using the approach of [4, Appendix I], the pdfs of $U_{i0,\max}$ and $U_{ij,\max}$, $i = 1, 2, \ldots, u$ after normalizing by $\overline{U}_{ij}^l = 4\xi N_0/u$ can be expressed as

$$f_{U_{i0,\max}}(x) = \frac{L}{1+\overline{\gamma}_0} \exp\left(-\frac{x}{1+\overline{\gamma}_0}\right) \cdot \left[1 - \exp\left(-\frac{x}{1+\overline{\gamma}_0}\right)\right]^{L-1},\ x \geq 0 \tag{13}$$

$$f_{U_{ij,\max}}(x) = (m_i - 1)\, L \exp(-x) \left[1 - \exp(-x)\right]^{(m_i-1)L-1},\ x \geq 0 \tag{14}$$

where $\overline{\gamma}_0 = E[\beta^2]\xi/(uN_0)$. The probability that the residue digit $r_i, i = 1, 2, \ldots, u$, is received correctly is simply the probability that $U_{i0,\max}$ exceeds $U_{ij,\max}$. Using the pdfs of (13) and (14), we can express the probability of r_i's being received correctly as

$$P_i(C) = \sum_{m=1}^{L} (-1)^{m+1} \binom{L}{m} \prod_{n=1}^{L(m_i-1)} \left(\frac{n}{n + \frac{m}{(1+\overline{\gamma}_0)}}\right). \tag{15}$$

Finally, the correct symbol probability $P_s(C)$ and the BER of $P_b(\epsilon)$ can be expressed according to (10) and (11).

We have obtained the expressions for the evaluation of the BER of the RNS-based system when EGC or SC receivers are considered. The results of [4] have shown that the BER performance of the RNS-based system can be improved by using RNS processing. Hence, let us now analyze the BER performance of the system with RNS processing using a similar method to that of [4], but over fading channels.

IV. Performance With RNS Processing

In order to evaluate the BER performance of the RNS-based system with the aid of RNS processing, as seen as in [4, Fig. 2], we first compute the pdfs of the RST under the hypothesis that the demodulator output for receiving residue digit r_i is correct (H_1) or in error (H_0). For the residue digit $r_i, i = 1, 2, \ldots, u$, the RST has been defined as $\lambda_i = {}^1\max\{\cdot\}/{}^2\max\{\cdot\}$ in [4], where ${}^1\max\{\cdot\}$ and ${}^2\max\{\cdot\}$ represent the (first) maximum and the "second maximum" in the variable set $\{U_{i0}, U_{i1}, \ldots, U_{i(m_i-1)}\}$, respectively, and where U_{ij} for $j = 0, 1, \ldots, m_i - 1$, represents the output after multipath combining. For EGC, U_{ij} is given by (5). Its normalized pdf is given by (6) when $j = 0$ or by (7), otherwise, remembering that the residue sequence (0, 0, ..., 0) was transmitted. However, for an L-branch diversity receiver with SC, we cannot directly use the branch outputs in order to invoke the RST, since there are L number of correlator outputs matched to the transmitted signal. In this paper, a two-stage maximum selection [5] is assumed in order to invoke the RST. In the first-stage maximum selection, the maximum of the L diversity components $\left\{U_{ij}^1, U_{ij}^2, \ldots, U_{ij}^L\right\}$ for each specific given i and j is selected. Explicitly, only one output is matched to the transmitted signal and $(m_i - 1)$ outputs are mismatched to the transmitted signal after this selection. Hence, the first-stage L-branch diversity selection outputs are expressed as

$$U_{ij} = \max\left\{U_{ij}^1, U_{ij}^2, \ldots, U_{ij}^L\right\} \tag{16}$$

for $i = 1, 2, \ldots, u$ and $j = 0, 1, \ldots, m_i - 1$. Assuming that the transmitted residue sequence is (0, 0, ..., 0), the normalized pdf of U_{i0} is given by (13), and the pdfs of U_{ij} with $j \neq 0$ are given by

$$f_{U_{ij}}(x) = L \exp(-x) \left[1 - \exp(-x)\right]^{L-1},\ x \geq 0 \tag{17}$$

for $j = 1, 2, \ldots, (m_i - 1)$.

In the second-stage maximum selection, the maximum of the first-stage outputs—namely, that of $(U_{i0}, U_{i1}, \ldots, U_{i(m_i-1)})$—is selected for demodulation. Simultaneously, the ratio of the maximum to the "second maximum" is computed in this stage, which will be used in the RNS processing. Note that using the above two-stage maximum selection, the probability that residue digit r_i is demodulated correctly is the same as in (15).

The pdfs of the maximum, the "second maximum," and their corresponding ratio λ_i under the correct and erroneous reception hypothesis of H_1 and H_0 can be derived using the pdfs of U_{ij}, which are given in [5] and [6] for the EGC and SC receiver.

Finally, the pdfs of λ_i under the correct and erroneous reception hypothesis of H_1 and H_0 can be expressed as

$$f_{\lambda_i}(y|H_1) = C_{H_1} \times g_{\lambda_i}(y|H_1),\ y \geq 1 \tag{18}$$

$$f_{\lambda_i}(y|H_0) = C_{H_0} \times g_{\lambda_i}(y|H_0),\ y \geq 1 \tag{19}$$

where $g_{\lambda_i}(y|H_1)$ and $g_{\lambda_i}(y|H_0)$ can be shown to obey the following.

For EGC

$$\begin{aligned} g_{\lambda_i}(y|H_1) =& y^{L-1} \int_0^{\infty} x^{2L-1} \exp\left(-x - \frac{xy}{1+\overline{\gamma}_0}\right) \\ & \cdot [1-\Psi(xy)]^{m_i-1}[1-\Psi(x)]^{m_i-2} \\ & \Psi\left(\frac{x}{1+\overline{\gamma}_0}\right) dx \end{aligned} \tag{20}$$

$$\begin{aligned} g_{\lambda_i}(y|H_0) =& y^{L-1} \int_0^{\infty} x^{2L-1} \exp(-xy)[1-\Psi(xy)]^{m_i-2} \\ & \cdot \left[1-\Psi\left(\frac{xy}{1+\overline{\gamma}_0}\right)\right] \Psi(x)[1-\Psi(x)]^{m_i-3} \\ & \cdot \left\{ \frac{1}{(1+\overline{\gamma}_0)^L} \exp\left(-\frac{x}{1+\overline{\gamma}_0}\right)[1-\Psi(x)] \right. \\ & + (m_i-2)\exp(-x) \\ & \left. \cdot \left[1-\Psi\left(\frac{x}{1+\overline{\gamma}_0}\right)\right] \right\} dx \end{aligned} \tag{21}$$

where the shorthand $\Psi(y)$ was defined as

$$\Psi(y) = \exp(-y) \sum_{k=0}^{L-1} \frac{y^k}{k!}. \tag{22}$$

For SC

$$\begin{aligned} g_{\lambda_i}(y|H_1) = & \int_0^{\infty} \left[\left(1-\exp\left(-\frac{xy}{1+\overline{\gamma}_0}\right)\right) \right. \\ & \left. \cdot (1-\exp(-x)) \right]^{L-1} \\ & \cdot [1-\Omega(xy)]^{m_i-1} \Omega\left(\frac{x}{1+\overline{\gamma}_0}\right) \\ & \cdot [1-\Omega(x)]^{m_i-2} x \exp\left(-x - \frac{xy}{1+\overline{\gamma}_0}\right) dx \end{aligned} \tag{23}$$

$$\begin{aligned} g_{\lambda_i}(y|H_0) = & \int_0^{\infty} [1-\exp(-xy)]^{L-1} \left[1-\Omega\left(\frac{xy}{1+\overline{\gamma}_0}\right)\right] \\ & \cdot [1-\Omega(xy)]^{m_i-2} \Omega(x) \cdot [1-\Omega(x)]^{m_i-3} \\ & \cdot \left\{ \frac{1}{1+\overline{\gamma}_0} \exp\left(-\frac{x}{1+\overline{\gamma}_0}\right) \right. \\ & \cdot \left[1-\exp\left(-\frac{x}{1+\overline{\gamma}_0}\right)\right]^{L-1} [1-\Omega(x)] \\ & + (m_i-2)\exp(-x)[1-\exp(-x)]^{L-1} \\ & \left. \cdot \left[1-\Omega\left(\frac{x}{1+\overline{\gamma}_0}\right)\right] \right\} \\ & \cdot x \exp(-xy) dx \end{aligned} \tag{24}$$

where the shorthand $\Omega(y)$ was defined as

$$\begin{aligned} \Omega(y) =& \sum_{k=1}^{L} (-1)^{k+1} \binom{L}{k} \exp(-ky) \\ =& 1-[1-\exp(-y)]^L. \end{aligned} \tag{25}$$

The parameters C_{H_1} and C_{H_0} in (18) and (19) can be obtained by integrating both sides of (18) and (19) from one to infinity, which arrive at

$$C_{H_1} = \frac{1}{\int_1^{\infty} g_{\lambda_i}(y|H_1)\, dy} \tag{26}$$

$$C_{H_0} = \frac{1}{\int_1^{\infty} g_{\lambda_i}(y|H_0)\, dy}. \tag{27}$$

We have obtained the probability distribution functions of λ_i, $i = 1, 2, \ldots, u$, under the hypothesis of H_1 and H_0 for EGC and SC. Let us now focus our attention on deriving the expression of the average BER by first estimating the correct symbol probability after the IRNST stage of [4, Fig. 2]. The average BER can be estimated using (11).

Let us now assume that an RRNS(u, v) code is introduced for residue digit protection. In the RNS-processing stage of Fig. 2, d ($d \leq u - v$) number of lowest reliability inputs of the RNS-processing unit—i.e., the d number of inputs with the lowest values of λ_i amongst the u inputs—are first dropped. Then the remaining residue digit errors may be corrected by the reduced RRNS$(u-d, v)$ decoding, as discussed previously in Part I. According to the analysis of [4], we know that an RRNS$(u-d, v)$ code can correct up to $t_{\max} = [(u-v-d)/2]$ residue digit errors and detect up to $(u-v-d)$ residue digit errors.

Let t represent the number of residue digit errors in the received RRNS(u, v) codeword, and let s ($s \leq d$) represent the number of residue digit errors discarded by dropping d number of the lowest reliability RNS-processing inputs in [4, Fig. 2] before RRNS$(u-d, v)$ decoding. Since an RRNS$(u-d, v)$ code can correct up to $t_{\max} = [(u-v-d)/2]$ residue digit errors [9], following the analysis of [4, Section V], the correct symbol probabilities of EGC and SC after IRNST can be treated according to the following three cases.

A. Error-Correction-Only RNS Processing

When error-correction-only RNS processing is used, the residue digit errors can be corrected by the RRNS(u, v) error-correction decoding, but in this case no lowest reliability RNS-processing inputs are dropped before decoding. Consequently, the correct symbol probability after IRNST can be expressed as

$$\begin{aligned} & P_s(C) \\ & = \sum_{t=0}^{t_{\max}} \left\{ \sum_{Q\binom{u}{t}} \left[\prod_{m=1}^{t} (1-P_{j_m}(C)) \prod_{n=1, n\neq m}^{u} P_{j_n}(C) \right] \right\} \end{aligned} \tag{28}$$

where $t_{\max} = [(u-v)/2]$, $\prod_{()=1}^{0}(\cdot) = 1$, while $P_{j_m}(C)$ and $P_{j_n}(C)$ are given by (9) or (15) for EGC or SC, respectively. Furthermore, $\{j_1, j_2, \ldots, j_u\}$ is a possible mapping of $\{1, 2, \ldots, u\}$ and $Q\binom{u}{t}$ represents that t out of u of the MLD outputs $\{U_1, U_2, \ldots, U_u\}$ were decided wrongly, i.e., t out of u residue digits are received in error before the RNS processing, but the other $(u-t)$ residue digits are error-free. All possible selections of t elements from $\{1, 2, \ldots, u\}$ are represented by

$$\sum_{Q\binom{u}{t}} \cdot$$

Similarly to Part I, here we briefly portray the relationship between the well-known RS codes and the less widespread RRNS codes. Specifically, if an RS coded system is considered, then $P_{j_m}(C) = P_{j_n}(C) = P_j(C)$ and

$$\sum_{Q\binom{u}{t}} = \binom{u}{t}.$$

Consequently, (28) is reduced to

$$P_s(C) = \sum_{t=0}^{t_{\max}} \binom{u}{t} [1 - P_j(C)]^t [P_j(C)]^{u-t}. \tag{29}$$

B. Error-Dropping-Only RNS Processing

For a receiver designed with error-dropping-only RNS processing, the symbol can be recovered correctly by the IRNST, even if there were residue digit errors, provided that the erroneous inputs are the lowest reliability inputs. Hence they are dropped during the RNS processing by dropping d number of its inputs, namely, those having the lowest values of λ_i. Hence, the correct symbol probability after IRNST can be expressed as

$$P_s(C) = \sum_{t=0}^{d} \left\{ \sum_{Q\binom{u}{t}} \left[\prod_{m=1}^{t} (1 - P_{j_m}(C)) \prod_{n=1, n\neq m}^{u} P_{j_n}(C) \right] \right\} \cdot P(d,t) \tag{30}$$

where $P(d,t)$ is the probability that t number of residue digit errors are successfully discarded by dropping d number of the lowest reliability inputs of the RNS-processing unit. Accordingly, $P(d,0) = 1$.

Let $A = \{\lambda_{m_1}, \lambda_{m_2}, \ldots, \lambda_{m_{(u-t)}}\}$ represent the ratio set for which the residue digits are received correctly, while $B = \{\overline{\lambda}_{n_1}, \overline{\lambda}_{n_2}, \ldots, \overline{\lambda}_{n_t}\}$ represent the ratio set for which the residue digits are received in error, where the overbar of λ_{n_j} is used to indicate the erroneous reception hypothesis of H_0. Then, the probability $P(d,t)$ in (30) can be expressed as shown in (31) at the bottom of the page, where $f_{\lambda_{m_{\{\cdot\}}}}(y|H_1)$ and $f_{\overline{\lambda}_{n_{\{\cdot\}}}}(x|H_0)$ are given by (18) and (19), respectively.

Note that if $f_{\overline{\lambda}_{n_{\{\cdot\}}}}(x|H_0)$ is approximated as a Dirac pulse function of $\delta(y-1)$—as discussed in Part I—then $P(d,t)$ is

$$P(d,t) = \sum_{h=0}^{d-t} \left\{ \sum_{Q\binom{t}{1} Q\binom{u-t}{h}} P\left(\underbrace{\lambda_{m_{i_1}} < \overline{\lambda}_{n_\mu}, \lambda_{m_{i_2}} < \overline{\lambda}_{n_\mu}, \ldots, \lambda_{m_{i_h}} < \overline{\lambda}_{n_\mu}}_{h}; \right.\right.$$
$$\underbrace{\lambda_{m_{j_1}} > \overline{\lambda}_{n_\mu}, \lambda_{m_{j_2}} > \overline{\lambda}_{n_\mu}, \ldots, \lambda_{m_{j_{(u-t-h)}}} > \overline{\lambda}_{n_\mu}}_{u-t-h};$$
$$\left.\left. \underbrace{\overline{\lambda}_{n_1} < \overline{\lambda}_{n_\mu}, \overline{\lambda}_{n_2} < \overline{\lambda}_{n_\mu}, \ldots, \overline{\lambda}_{n_{\mu-1}} < \overline{\lambda}_{n_\mu}, \overline{\lambda}_{n_{\mu+1}} < \overline{\lambda}_{n_\mu}, \ldots, \overline{\lambda}_{n_t} < \overline{\lambda}_{n_\mu}}_{t-1} \right) \right\}$$
$$= \sum_{h=0}^{d-t} \left\{ \sum_{Q\binom{t}{1} Q\binom{u-t}{h}} \int_0^\infty \left[\prod_{\eta=1}^{h} \int_0^x f_{\lambda_{m_{i\eta}}}(y|H_1) dy \right] \left[\prod_{\nu=1}^{u-t-h} \int_x^\infty f_{\lambda_{m_{j\nu}}}(y|H_1) dy \right] \right.$$
$$\left. \cdot \left[\prod_{\zeta=1, \zeta\neq\mu}^{t} \int_0^x f_{\overline{\lambda}_{n_\zeta}}(y|H_0) dy \right] f_{\overline{\lambda}_{n_\mu}}(x|H_0) dx \right\} \tag{31}$$

reduced to [4, (25)] when $\int_0^1 f_{\overline{\lambda}_{n_\zeta}}(y|H_0)dy = 1/2$ is assumed. Furthermore, if an RS coded system is considered, (31) can be simplified to

$$P(d,t) = \sum_{h=0}^{d-t} \binom{t}{1} \binom{u-t}{h} \cdot \int_0^\infty \left[\int_0^x f_{\lambda_M}(y|H_1)\,dy\right]^h \cdot \left[\int_x^\infty f_{\lambda_M}(y|H_1)\,dy\right]^{u-t-h} \cdot \left[\int_0^x f_{\overline{\lambda}_M}(y|H_0)\,dy\right]^{t-1} f_{\overline{\lambda}_M}(x|H_0)dx. \quad (32)$$

C. Error-Dropping-and-Correction RNS Processing

Similarly to our discussions in [4, Section V], the correct symbol probability after IRNST can be expressed as

$$P_s(C) = \sum_{t=0}^{d+t_{\max}} \left\{ \sum_{Q\binom{u}{t}} \left[\prod_{m=1}^{t}(1-P_{j_m}(C)) \cdot \prod_{n=1,n\neq m}^{u} P_{j_n}(C)\right]\right\} \cdot P(s \geq t - t_{\max}) \quad (33)$$

where the term $P_{j_m}(C)$ is the correct reception probability of r_{j_m} given by (9) or (15) for EGC or SC, respectively. The term $P(s \geq t - t_{\max})$ in (33) represents the probability that the number of discarded residue digit errors is not less than $t - t_{\max}$. Accordingly, $P(s \geq t - t_{\max}) = 1$, if $t \leq t_{\max}$. By contrast, when $t > t_{\max}$, it can be expressed as shown in (34) at the bottom of the page, where $\lambda_{m\{\cdot\}}$ and $\overline{\lambda}_{n\{\cdot\}}$ are from ratio sets A and B, which were defined previously. Note that if $t_{\max} = 0$, then $P(s \geq t - t_{\max})$ of (34) becomes equivalent to $P(d,t)$ of (31). Furthermore, if $f_{\overline{\lambda}_i}(x|H_0)$ is approximated as a Dirac pulse function of $\delta(x-1)$—as discussed in Part I—then $P(s \geq t - t_{\max})$ is reduced to (27) of [4], upon assuming that $\int_0^1 f_{\overline{\lambda}_{n_\zeta}}(y|H_0)dy = \int_1^\infty f_{\overline{\lambda}_{n_\zeta}}(y|H_0)dy = 1/2$. Furthermore, if an RS coded system is considered, (34) can be simplified to

$$P(s \geq t - t_{\max}) = \sum_{h=0}^{d+t_{\max}-t} \binom{t}{1}\binom{u-t}{h}\binom{t}{t_{\max}} \cdot \int_0^\infty \left[\int_0^x f_{\lambda_M}(y|H_1)\,dy\right]^h \cdot \left[\int_x^\infty f_{\lambda_M}(y|H_1)\,dy\right]^{u-t-h} \cdot \left[\int_x^\infty f_{\overline{\lambda}_M}(y|H_0)\,dy\right]^{t_{\max}} \cdot \left[\int_0^x f_{\overline{\lambda}_M}(y|H_0)\,dy\right]^{t-t_{\max}-1} \cdot f_{\overline{\lambda}_M}(x|H_0)\,dx. \quad (35)$$

We have analyzed the performance of the proposed RNS-based orthogonal signaling system when noncoherent demod-

$$P(s \geq t - t_{\max}) = \sum_{h=0}^{d+t_{\max}-t} \left\{ \sum_{Q\binom{t}{1}} \sum_{Q\binom{u-t}{h}} \sum_{Q\binom{t}{t_{\max}}} P\left(\underbrace{\lambda_{m_{i_1}} < \overline{\lambda}_{n_\mu}, \lambda_{m_{i_2}} < \overline{\lambda}_{n_\mu}, \ldots, \lambda_{m_{i_h}} < \overline{\lambda}_{n_\mu}}_{h}; \underbrace{\lambda_{m_{j_1}} > \overline{\lambda}_{n_\mu}, \lambda_{m_{j_2}} > \overline{\lambda}_{n_\mu}, \ldots, \lambda_{m_{j_{(u-t-h)}}} > \overline{\lambda}_{n_\mu}}_{u-t-h}; \underbrace{\overline{\lambda}_{n_{k_1}} > \overline{\lambda}_{n_\mu}, \overline{\lambda}_{n_{k_2}} > \overline{\lambda}_{n_\mu}, \ldots, \overline{\lambda}_{n_{k_{t_{\max}}}} > \overline{\lambda}_{n_\mu}}_{t_{\max}}; \underbrace{\overline{\lambda}_{n_{l_1}} < \overline{\lambda}_{n_\mu}, \overline{\lambda}_{n_{l_2}} < \overline{\lambda}_{n_\mu}, \ldots, \overline{\lambda}_{n_{l_{(t-t_{\max}-1)}}} < \overline{\lambda}_{n_\mu}}_{t-t_{\max}-1}; \right) \right\}$$

$$= \sum_{h=0}^{d+t_{\max}-t} \left\{ \sum_{Q\binom{t}{1}} \sum_{Q\binom{u-t}{h}} \sum_{Q\binom{t}{t_{\max}}} \int_0^\infty \left[\prod_{\eta=1}^{h}\int_0^x f_{\lambda_{m_{i_\eta}}}(y|H_1)dy\right] \left[\prod_{\nu=1}^{u-t-h}\int_x^\infty f_{\lambda_{m_{j_\nu}}}(y|H_1)dy\right] \cdot \left[\prod_{\kappa=1}^{t_{\max}}\int_x^\infty f_{\overline{\lambda}_{n_{k_\kappa}}}(y|H_0)dy\right] \left[\prod_{\zeta=1}^{t-t_{\max}-1}\int_0^x f_{\overline{\lambda}_{n_{l_\zeta}}}(y|H_0)dy\right] f_{\overline{\lambda}_{n_\mu}}(x|H_0)dx \right\} \quad (34)$$

ulation, diversity reception with EGC or SC, and RNS processing were considered. However, for wireless communications, powerful forward error correction (FEC) is required in order to maintain high-reliability communications. Hence let us now discuss the structure and the performance of the proposed RNS-based orthogonal system in conjunction with a concatenated RS code.

V. Performance With Concatenated Error orrection

Concatenated coding [7], [11]–[13] is a technique of combining relatively simple channel codes in order to form a powerful coding system for achieving a high performance and large coding gain with reduced decoding complexity. In practical applications, traditionally the inner code is usually a relatively short binary block code or a binary convolutional code with relatively short constraint length. The outer code is usually an RS code with symbols from a Galois field GF(2^m).

The family of RRNS codes constitutes a class of maximum–minimum distance codes [9] akin to RS codes. RRNS codes can provide a powerful error-correction and error-detection capability that is similar to that of RS codes, but the inherent parallel structure of the RNS arithmetic, the associated independent residue processing, and the availability of convenient decoding algorithms render RRNS codes an attractive alternative for use as inner codes. Short RRNS codes can be combined with RS codes, where the former is used as the inner code, in order to form a concatenated RS-RRNS code. Furthermore, as we have shown in this paper, it is possible to realize high-bit-rate communication using an RNS arithmetic by combining the RNS with highly efficient modulation and demodulation schemes, such as the RNS-based M-ary orthogonal signaling scheme discussed in this paper.

Using an RS-RRNS concatenated code, after RRNS inner decoding, the symbol error probability is typically decreased to a degree that may maximize the external RS coding gain. Hence the average symbol error probability is further decreased to the required degree using RS decoding. In addition, the error-detection capability of the RRNS code can provide symbol error information or erasure information for the RS outer decoding. Consequently, the effectiveness of the RS code utilizing error-and-erasure correction decoding can be enhanced upon exploiting the explicit error-detection capability of the inner code, since in this case the error positions are known by the RS decoder. Hence all the RS syndrome-equations can be used to determine a doubled number of RS symbol error magnitudes in comparison to the scenario where there is no erasure—i.e., no error position information is available—requiring the determination of both the error positions and the magnitudes.

Let N_c and K_c be the length of an RS code and the number of original information symbols, respectively. If ideal interleaving of the RS code symbols is assumed, then after error-correction-only decoding, the resulting symbol error probability after RS hard decision decoding is approximately given by [14]

$$P_{s,d}(\epsilon) \approx \frac{1}{N_c} \sum_{i=[(N_c-K_c)/2]+1}^{N_c} i \binom{N_c}{i} P_t^i (1-P_t)^{N_c-i} \tag{36}$$

where P_t represents the probability of a random symbol error after RRNS decoding, which is given, for example, by $(1 - P_s(C))$, depending on the RRNS structure and decoding algorithm used. If RS symbol erasure information can be provided by the RRNS decoding, error-and-erasure correction RS decoding can be applied. Consequently, the resulting symbol error probability after RS decoding is approximately given by [16]

$$P_{s,d}(\epsilon) \approx \frac{1}{N_c} \sum_{i=0}^{N_c} \sum_{j=j_0(i)}^{N_c-i} (i+j) \binom{N_c}{i} \binom{N_c-i}{j} \cdot P_t^i P_e^j (1-P_t-P_e)^{N_c-i-j} \tag{37}$$

where $j_0(i) = \max\{0, N_c - K_c + 1 - 2i\}$, while P_t and P_e are the probability of a random symbol error and a symbol erasure after RRNS decoding. Note that $P_{s,d}(\epsilon)$ in (37) is the average joint probability of uncorrectable random symbol errors and symbol erasures—in other words, the average probability of decoding failure.

P_t and P_e can be computed according to the RRNS decoding algorithm discussed previously. However, for an error-detection-only RRNS code, P_t and P_e can be computed by [8]

$$P_t \approx \frac{1}{M_r} P_s(\epsilon) \tag{38}$$

$$P_e \approx \frac{M_r - 1}{M_r} P_s(\epsilon) \tag{39}$$

where $P_s(\epsilon)$ is the average symbol error probability before RRNS decoding, i.e., before RNS processing; and $M_r = \prod_{i=1}^{u-v} m_{v+i}$ is the product of the redundant moduli. From (38) and (39), we infer that after RRNS decoding, most RS error symbols will be marked as erasure. Let us now evaluate the BER performance of the proposed RNS-based orthogonal system numerically.

VI. Numerical Results and Analysis

In this section, we first consider the distribution of the RST decision variable $\lambda_i, i = 1, 2, \ldots, u$, over Rayleigh fading multipath channels. Then the average BER is evaluated as a function of the average SNR per bit, which is obtained by computing $\overline{\gamma}_b = L_p u \overline{\gamma}_0 / (\log_2 \prod_{i=1}^{v} m_i)$ for all systems described above.

Figs. 3 and 4 show the pdfs of the RST under the hypotheses H_1 and H_0 for EGC (Fig. 3) and SC (Fig. 4) for different values of m_i and for SNR per bit values of $\gamma_b = 5, 8$, and 15 dB. In the computations, we assumed that there were $L_p = 3$ resolvable multipath components at the receiver, but only $L = 2$ of them were combined for the sake of maintaining a low complexity. Our results were computed according to (18) and (19) associated with (20) and (21) for EGC and associated with (23) and (24) for SC when the parameter m_i took values of 8, 32, 128. From the results, we observe that for a given value of m_i, the peak of the distribution of $f_{\lambda_i}(y|H_1)$ will shift to the right for both EGC and SC, while $f_{\lambda_i}(y|H_0)$ is distributed essentially around $y \approx 1$, but at a point slightly higher than $y = 1$. The peak of the distribution of $f_{\lambda_i}(y|H_0)$ becomes lower as the SNR per bit increases from 5 to 15 dB. However, for a given value of γ_b, the peaks of the distributions of $f_{\lambda_i}(y|H_1)$ and $f_{\lambda_i}(y|H_0)$ become higher when increasing the value of m_i. Especially for the distribution $f_{\lambda_i}(y|H_0)$, the peak changes significantly when

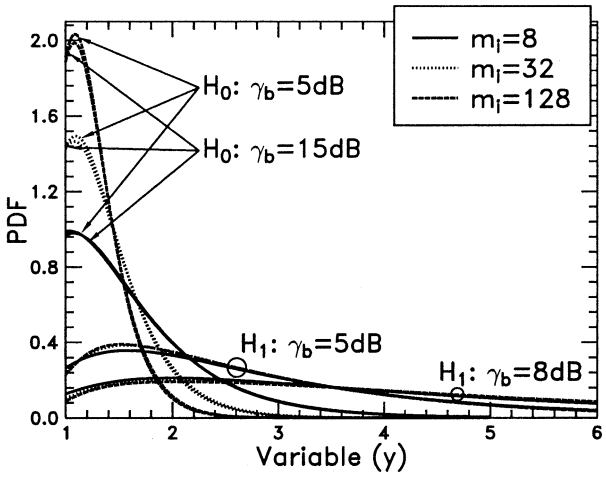

Fig. 3. EGC: the pdf of $\lambda_i = {}^1\max\{\cdot\}/{}^2\max\{\cdot\}$ according to (18) and (19) associated with (20) and (21) under the assumptions of H_1 and H_0 using the moduli of $m_i = 8, 32, 128$, $L_p = 3$, $L = 2$, and Rayleigh fading channel SNR/bit of $\gamma_b = 5, 8$, and 15 dB.

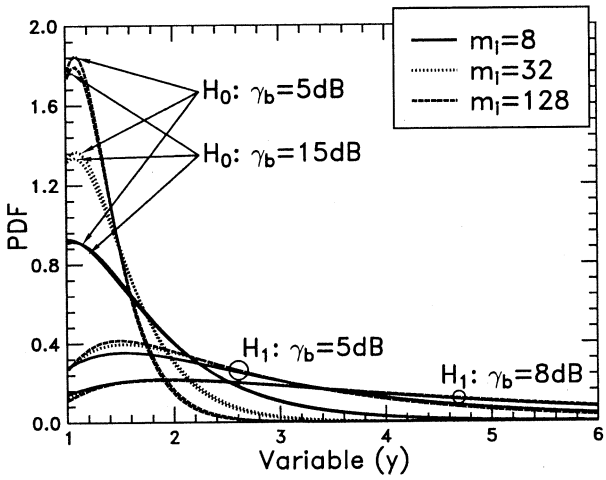

Fig. 4. SC: the pdf of $\lambda_i = {}^1\max\{\cdot\}/{}^2\max\{\cdot\}$ according to (18) and (19) associated with (23) and (24) under the assumptions of H_1 and H_0 using the moduli of $m_i = 8, 32, 128$, $L_p = 3$, $L = 2$, and Rayleigh fading channel SNR/bit of $\gamma_b = 5, 8$, and 15 dB.

changing the value of m_i. Observe furthermore that the pdfs of the RST decision variable λ_i, $i = 1, 2, \ldots, u$, are similar for both EGC and SC, as shown in Figs. 3 and 4.

In Fig. 5, we used SC as an example to evaluate the effect of the number of multipath components at different SNRs per bit on the distribution of $f_{\lambda_i}(y|H_1)$ and $f_{\lambda_i}(y|H_0)$. We assumed that $m_i = 32$, $L_p = 5$, and that the receiver could combine $L = 1, 2, 3$ multipath components. The results show that for a given SNR per bit, when increasing the number of the multipath components L that the receiver combined, the peak of the distribution $f_{\lambda_i}(y|H_1)$ shifts to the right, while the peak of the distribution of $f_{\lambda_i}(y|H_0)$ is increased. The above results suggest that an erroneous input to the RNS processing of a receiver using more multipath components will be dropped with a higher probability than that of a receiver using fewer multipath components, since the dropping failure depends on the area of the overlapping region of $f_{\lambda_i}(y|H_1)$ and $f_{\lambda_i}(y|H_0)$ at a given SNR per bit.

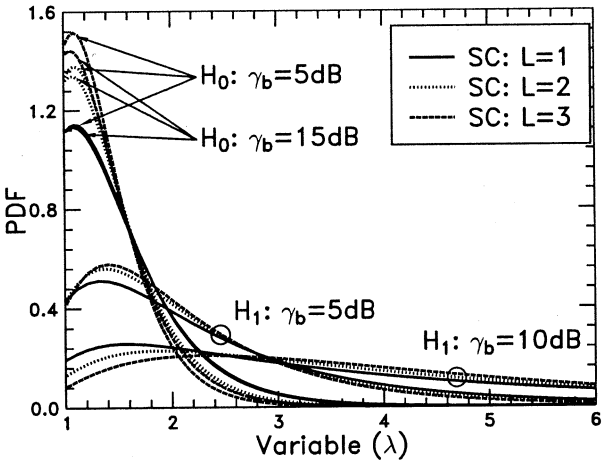

Fig. 5. SC: the pdf of $\lambda_i = {}^1\max\{\cdot\}/{}^1\max\{\cdot\}$ according to (18) and (19) associated with (23) and (24) under the assumptions of H_1 and H_0 using the moduli of $m_i = 32$, $L_p = 5$ and $L = 1, 2, 3$, and Rayleigh fading channel SNR/bit of $\gamma_b = 5, 15$, and 20 dB.

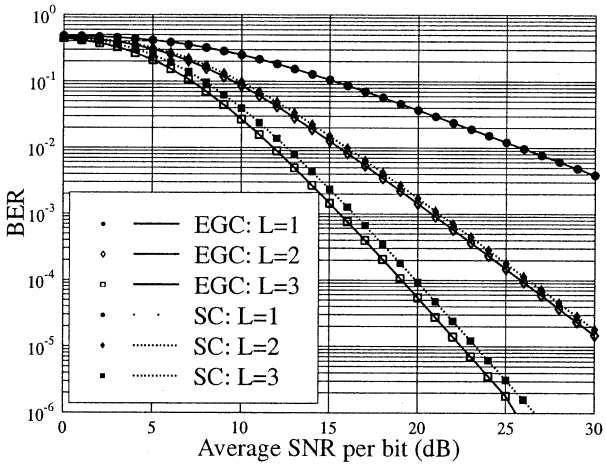

Fig. 6. EGC, SC: BER versus average SNR per bit for the RNS-based orthogonal signaling system with three moduli $m_1 = 7$, $m_2 = 8$, and $m_3 = 9$. $L_p = 3$ evaluated from (9), (11), and (15).

Fig. 6 shows the BER for the EGC and SC schemes with $L = 1, 2, 3$ upon evaluating (9)–(11) for EGC and (11) and (15) for SC. We assumed that there were $L_p = 3$ resolvable multipath components at the receiver. A nonredundant RNS-based system with its moduli taking values of $m_1 = 7, m_2 = 8$, $m_3 = 9$ was considered. As expected, both the EGC and the SC schemes provide dramatic BER improvements for moderate to high SNRs per bit when the number of combined diversity paths L increases. Furthermore, the results show that the EGC scheme has a lower BER than the SC scheme. Again, this is because EGC is the optimal diversity combining scheme for a noncoherent demodulation technique.

In Fig. 7, which is related to the EGC scheme, and in Fig. 8 characterizing the SC scheme, we evaluated the BER performance of a system employing RNS processing without redundancy, or using one redundant modulus with one lowest reliability input of the RNS processing discarded, which we denote as $d = 0$ and $d = 1$, respectively. In the related probability expressions of (31), moduli taking values of 29, 31, 32, 33, 35, 37, and 41 were used. There were $L_p = 3$ resolvable

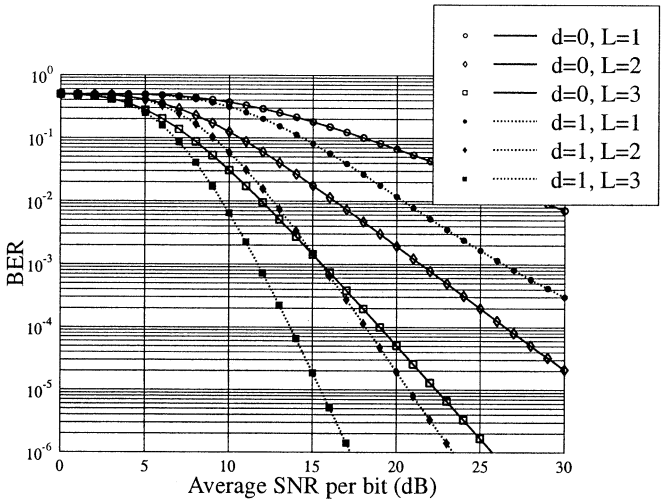

Fig. 7. EGC: BER versus average SNR per bit for the RNS-based orthogonal signaling system with seven moduli—$m_1 = 29, m_2 = 31, m_3 = 32, m_4 = 33, m_5 = 35, m_6 = 37, m_7 = 41$—and $L_p = 3$, where d is the number of lowest reliability inputs of RNS processing dropped, evaluated from (11) and (30).

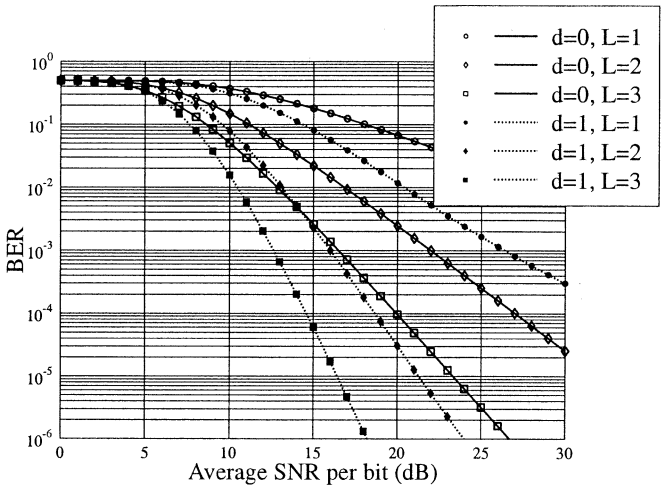

Fig. 8. SC: BER versus average SNR per bit for the RNS-based orthogonal signaling system with seven moduli—$m_1 = 29, m_2 = 31, m_3 = 32, m_4 = 33, m_5 = 35, m_6 = 37, m_7 = 41$—and $L_p = 3$, where d is the number of lowest reliability inputs of RNS processing dropped, evaluated from (11) and (30).

paths, and $L = 1, 2$, or 3 paths were actually combined in the receiver using an EGC or SC scheme. The results show that when the RNS is designed with redundant moduli, the BER performance of both the EGC and the SC scheme is substantially improved. Taking $L = 2, 3$ paths as examples, the EGC scheme can achieve a BER of 10^{-4} at SNRs per bit of 18 or 13.5 dB when one lowest reliability input of the RNS processing is dropped during the RNS processing, shown by the $d = 1, L = 2$ and $d = 1, L = 3$ curves. However, if the RNS-based system is designed without redundancy, an average of 26 or 19 dB SNR per bit is required for the EGC scheme using $L = 2$ or $L = 3$ to achieve the BER of 10^{-4}. This implies that we can obtain about 8 or 5.5 dB gain at $P_b(\epsilon) = 10^{-4}$ by using one lowest reliability RNS-processing input dropping for $L = 2$ or 3, respectively. Similarly, the SC scheme using $L = 2$ or 3 can achieve a BER of 10^{-4} at SNRs per bit of 18.5 or 14.5 dB and obtain about 8

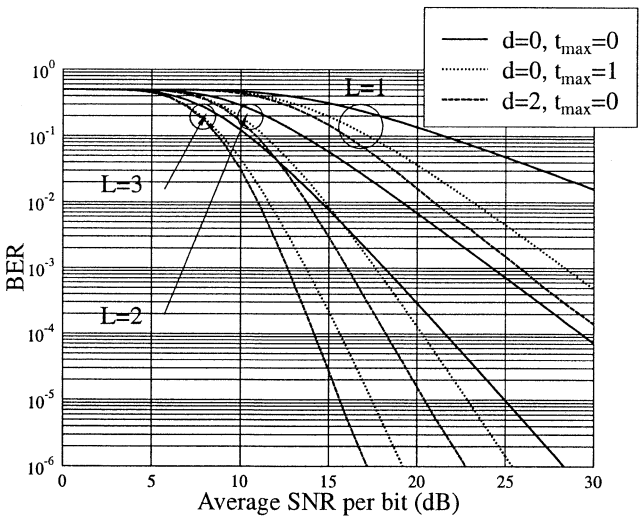

Fig. 9. EGC: BER versus average SNR per bit for the RNS-based orthogonal signaling system with ten moduli—$m_1 = 29, m_2 = 31, m_3 = 35, m_4 = 36, m_5 = 37, m_6 = 41, m_7 = 43, m_8 = 47, m_9 = 53, m_{10} = 59$—and $L_p = 5$, where $t_{\max}$ is the number of errors corrected by RRNS$(u - d, v)$ and d is the number of lowest reliability inputs of RNS processing dropped, evaluated from (11) and (33). $L = 1, 2, 3$.

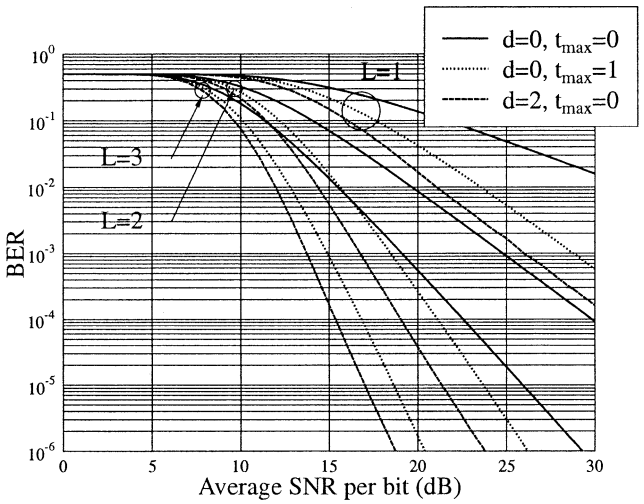

Fig. 10. SC: BER versus average SNR per bit for the RNS-based orthogonal signaling system with ten moduli—$m_1 = 29, m_2 = 31, m_3 = 35, m_4 = 36, m_5 = 37, m_6 = 41, m_7 = 43, m_8 = 47, m_9 = 53, m_{10} = 59$—and $L_p = 5$, where $t_{\max}$ is the number of errors corrected by RRNS$(u - d, v)$ and d is the number of lowest reliability inputs of RNS processing dropped, evaluated from (11) and (33). $L = 1, 2, 3$.

or 5.5 dB gain at $P_b(\epsilon) = 10^{-4}$ by using one lowest reliability input dropping for $L = 2$ or 3, respectively. The coding gains observed in Figs. 7–11 are summarized in Table I.

Similarly to Figs. 7 and 8, in Figs. 9 and 10, we evaluated the BER performance of a ten-moduli RNS-based orthogonal signaling system using EGC or SC schemes when $d = 2$ lowest reliability inputs were dropped or $t_{\max} = 1$ residue digit error correction RNS processing was considered. Obviously, these two RNS-based systems used the same number of redundant moduli and had the same information rate. The parameters related to these investigations were $m_1 = 29, m_2 = 31, m_3 = 35, m_4 = 36, m_5 = 37, m_6 = 41, m_7 = 43, m_8 = 47, m_9 = 53, m_{10} = 59$, and $L_p = 5$. We notice that the BER

TABLE I
SUMMARY OF CODING GAIN ACHIEVED IN FIGS. 7–10

RNS-processing Mode	*k (bits)*	*Values of Moduli*	*EGC or SC*	L_p	L	*Coding gain (dB)*	
						1×10^{-3}	1×10^{-6}
One redundant modulus and lowest-reliability input dropping	*30*	$m_1 = 29, m_2 = 31, m_3 = 32,$ $m_4 = 33, m_5 = 35, m_6 = 37,$ $m_7 = 41$	*EGC*	*3*	*2*	6	> 10
				3	*3*	3.5	8.5
			SC	*3*	*2*	6	> 10
				3	*3*	3.5	8.5
Two redundant moduli and lowest-reliability input dropping	*41*	$m_1 = 29, m_2 = 31, m_3 = 35,$ $m_4 = 36, m_5 = 37, m_6 = 41,$ $m_7 = 43, m_8 = 47, m_9 = 53$ $m_{10} = 59$	*EGC*	*5*	*2*	8	> 11
				5	*3*	6	11
			SC	*5*	*2*	8	> 11
				5	*3*	6	11
Two redundant moduli and one residue digit error correction	*41*	$m_1 = 29, m_2 = 31, m_3 = 35,$ $m_4 = 36, m_5 = 37, m_6 = 41,$ $m_7 = 43, m_8 = 47, m_9 = 53$ $m_{10} = 59$	*EGC*	*5*	*2*	6.5	> 9
				5	*3*	4.5	9
			SC	*5*	*2*	6.5	> 9
				5	*3*	4.5	9

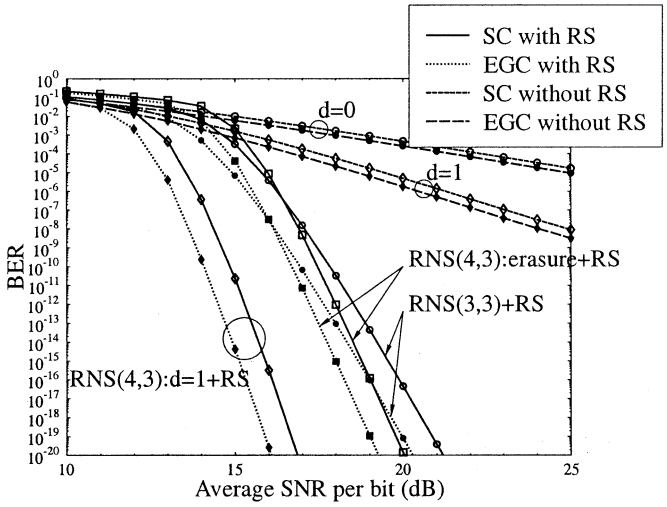

Fig. 11. EGC, SC: BER versus average SNR per bit for the RNS-based orthogonal signaling system using concatenated coding when moduli $m_1 = 5$, $m_2 = 7$, $m_3 = 8$ are employed for RNS(3,3), $m_1 = 5, m_2 = 7, m_3 = 8$, $m_4 = 9$ for RRNS(4,3) and RS(255 223), $L_p = 5$, $L = 3$ are assumed, d is the number of lowest reliability inputs of RNS processing dropped, and erasure represents that RS symbol erasure information obtained from the RRNS(4,3) decoding.

of the RNS-based system with the two lowest reliability inputs of the RNS processing discarded is lower than that of the system with one residue digit error-correction-based RNS-processing, when the same number of multipath components are combined in the receiver. Specifically, the EGC scheme with two lowest reliability inputs dropped requires 2 or 1.5 dB less bit-SNR than the system with one residue digit error correction for achieving a BER of 10^{-4} when $L = 2$ or $L = 3$ multipath components are combined in the receiver, respectively. The results imply that for a ten-moduli RNS-based system, RNS processing using lowest reliability dropping is a highly effective method of improving the system's BER performance. Furthermore, the complexity of the RRNS(10,8) decoding of dropping two of the lowest reliability inputs of the RNS processing is lower than that of the RRNS(10,8) one residue digit error-correction decoding.

In Fig. 11, we evaluated the BER performance of the RNS-based orthogonal signaling system when additional concatenated RS-coding was introduced. Specifically, an outer RS(255, 223) code over Galois field GF(2^8) using 8-bit symbols was invoked. This RS(255, 223) scheme has been proposed in the Consultative Committee for Space Data System standard as an outer code combined with a half-rate constraint-length $K = 7$ inner convolutional code for data protection [17]. Two decoding techniques—error correction only and error and erasure correction—were assumed, depending on the inner RRNS decoding. An 8-bit symbol was assumed to be transmitted per symbol period. The symbol erasure information—when required—was provided by the RRNS error-detection decoding. Since 8 bits were transmitted per symbol period, hence for a nonredundant RNS-based system, the moduli of $m_1 = 5, m_2 = 7, m_3 = 8$ were appropriate for transmitting the 8-bit symbol, since $5 \cdot 7 \cdot 8 = 280 > 256 = 2^8$. However, for this nonredundant RNS-based system, the symbol errors were corrected solely by the outer RS(255 223) code. The modulus values for the concatenated RRNS-based system can be selected similarly, which were $m_1 = 5$, $m_2 = 7$, $m_3 = 8$, and $m_4 = 9$ for the RRNS(4,3) code with $d = 1$ lowest reliability input of the RNS processing being dropped. Similarly, $m_1 = 5$, $m_2 = 7$, $m_3 = 8$, and $m_4 = 9$ were used for the RRNS(4,3) scheme with RRNS error-detection decoding, i.e., providing erasure information for the outer decoding by the RRNS decoding. The other parameters related to our proposed systems were $L_p = 5$, $L = 3$.

From the results of Fig. 11, we observe that the BER performance of the proposed system is dramatically improved by using the RS-RRNS concatenated coding for both the EGC and SC combining schemes. For example, for the receiver with EGC at an average bit-SNR of 15 dB, the average BER of 6×10^{-3} for the nonredundant RNS(3,3) system is first

decreased to 7.1×10^{-4} using the RRNS(4,3) scheme with one lowest reliability input of the RNS processing being dropped. It is further decreased to about 4.2×10^{-15} using RS(255 223) error-correction-only decoding. By contrast, without the inner RRNS(4,3)-based RNS processing, the average BER after RS(255 223) decoding can reach about 6.9×10^{-6}. Similar results can be obtained for the receiver using the SC scheme, but it is obvious that the SC combining technique is not as effective for the noncoherent receiver as the EGC scheme, which was noted previously. Furthermore, from the figures, we notice that using RRNS error detection and by providing erasure information for the outer RS decoding, the BER performance is improved less dramatically than by using RNS processing with the lowest reliability input of the RNS processing discarded and additionally using the RS error-correction-only decoding. This phenomenon can be explained as follows. Using lowest reliability input dropping, most erroneously received RS symbols are successfully recovered after inner decoding. Consequently, this decreased the number of erroneous RS symbols to be corrected by the RS decoder. However, if the inner RNS decoding is only used to provide erasure information for the outer RS decoding, the sum of erroneous and erasured symbols may exceed the RS codec's error-and-erasure correction capability, although RS decoding using error-and-erasure correction can correct more erroneous and erasured symbols than RS error-correction-only decoding without erasure information. For example, if the error probability of each residue digit concerning the above computations is less than 0.25, then the average erroneous number of residue digits in RRNS(4,3) is less than one. Hence, the erroneous residue digit can be typically dropped by the RNS processing using one lowest reliability input dropping. Consequently, there are very few erroneous symbols in the RS code. However, when using error-detection-only inner decoding, the previously dropped erroneous residues will now result in erased RS symbols. Consequently, the number of RS symbol errors often exceeds the error-and-erasure correction capability of the outer RS code.

Again, the coding gains achieved in Figs. 7–10 were summarized in Table I, where $k = [\log_2 \prod_{i=1}^{v} m_i]$ is the number of bits of the transmitted symbol represented by the related RRNS. Note that using RS-RRNS concatenated coding constituted by inner decoding employing lowest reliability input dropping and outer decoding invoking error-correction-only decoding, an additional 2- or 7-dB gain can be achieved at average BERs of 10^{-3} or 10^{-6}, respectively.

VII. Conclusions

In this paper, we have presented a novel parallel transmission technique that uses a set of orthogonal signals and associated correlator, which are processed according to the principles of RNS arithmetic algorithms. This technique is amenable to the transmission of signals having a high number of bits per symbol, while using a relatively low number of orthogonal signals. Therefore, it is useful for high-bit-rate communications. We have discussed the characteristics of the RNS arithmetic and how these special characteristics affect the communications performance in AWGN and in multipath Rayleigh fading channels. Based on the independence and on the equal weight properties of the residue digits of an RNS, a novel receiver for receiving RNS arithmetic-based orthogonal signals has been designed. In this novel receiver, an RRNS code can be decoded by first discarding a number of the lowest reliability symbols according to the so-called ratio statistic test—which is computed as the ratio of the (first) maximum to the "second maximum" of the inputs of RNS processing—and then decoding the reduced and simultaneously simplified RRNS code. Concatenated coding techniques have been discussed in a dispersive multipath fading scenario. The concatenated coding performance in conjunction with an RS code as the outer code and the RRNS code as the inner code has been evaluated both analytically and numerically. Our future work is focused on the design and performance evaluation of soft-decision-based adaptive RNS schemes, while the simulation-based verification of the analysis was the topic of [18].

References

[1] L. M. A. Jalloul and J. K. Holtzman, "Performance analysis of DS-CDMA with noncoherent M-ary orthogonal modulation in multipath fading channels," *IEEE J. Select. Areas Commun.*, vol. 12, pp. 862–870, June 1994.

[2] G. Chyi, J. G. Proakis, and C. M. Keller, "On the symbol error probability of maximum-selection diversity reception schemes over a rayleigh fading channel," *IEEE Trans. Commun.*, vol. 37, pp. 79–83, Jan 1989.

[3] J. G. Proakis, *Digital Communications*, 4th ed. New York: McGraw-Hill, 2000.

[4] L. L. Yang and L. Hanzo, "Performance of a residue number system based parallel communication system using orthogonal signaling: Part I—System outline," *IEEE Trans. Veh. Technol.*, vol. 51, pp. 1528–1540, Nov. 2002.

[5] L.-L. Yang, K. Yen, and L. Hanzo, "A Reed-Solomon coded DS-CDMA system using noncoherent M-ary orthogonal modulation over multipath fading channels," *IEEE J. Select. Areas Commun.*, vol. 18, pp. 2240–2251, Nov. 2000.

[6] L.-L. Yang and L. Hanzo, "Performance analysis of coded M-ary orthogonal signaling using errors-and-erasures decoding over frequency-selective fading channels," *IEEE J. Select. Areas Commun.*, vol. 19, pp. 211–221, Feb. 2001.

[7] ——, "Performance of residue number system based DS-CDMA over multipath fading channels using orthogonal sequences," *Eur. Trans. Telecommun.*, vol. 9, pp. 525–536, Nov.–Dec. 1998.

[8] K. W. Watson, "Self-checking computations using residue arithmetic," *Proc. IEEE*, vol. 54, pp. 1920–1931, Dec. 1966.

[9] H. Krishna and J. D. Sun, "On theory and fast algorithms for error correction in residue number system product codes," *IEEE Trans. Comput.*, vol. C-42, pp. 840–852, July 1993.

[10] S. Lin and D. J. Costello, *Error Control Coding-Fundamentals and Applications*, NJ: Prentice-Hall, 1983.

[11] G. D. Forney Jr., *Concatenated Codes*. Cambridge, MA: MIT Press, 1966.

[12] T. Kasami, "A concatenated coded modulation scheme for error control," *IEEE Trans. Commun.*, vol. 38, pp. 752–763, June 1990.

[13] ——, "On bit-error probability of a concatenated coding scheme," *IEEE Trans. Commun.*, vol. 45, pp. 536–543, June 1990.

[14] L. B. Milstein, R. B. Pickholtz, and D. L. Schilling, "Optimization of the processing gain of an FSK-FH system," *IEEE Trans. Commun.*, vol. COM-28, pp. 1062–1069, July 1980.

[15] W. K. Jenkins and E. J. Altman, "Self-checking properties of residue number error checkers based on mixed radix conversion," *IEEE Trans. Circuits Syst.*, vol. 35, pp. 159–167, Feb. 1988.

[16] C. W. Helstrom, *Probability and Stochastic Processes for Engineerings*, 2nd ed. New York: Macmillan, 1991.

[17] "Consultative committee for space data system," in *Recommendation for Space Data System Standard: Telemetry Channel Coding "Blue Book"*, 1984.

[18] K. Yen, L.-L. Yang, and L. Hanzo, "Residual number system assisted CDMA—A new system concept," in *Proc. ACTS'99 Summit*, Sorrento, Italy, June 8–11, 1999, pp. 177–182.

Lie-Liang Yang (M'98–SM'02) received the B.Eng. degree in communication engineering from Shanghai TieDao University, Shanghai, China, in 1988 and the M.S. and Ph.D. degrees in communications and electronics from Northern Jiaotong University, Beijing, China, in 1991 and 1997, respectively.

From 1991 to 1993, he was a Lecturer in the Department of Electrical Engineering, East-China Jiaotong University, China. From 1993 to 1997, he was with the Modern Communications Research Institute, Northern Jiaotong University, China. From June to December 1997, he was a Visiting Scientist at the Institute of Radio Engineering and Electronics, Academy of Sciences of the Czech Republic. Since December 1997, he has been with the Communication Group, Department of Electronics and Computer Science, University of Southampton, U.K., where he has been involved in researching various error-correction coding, modulation, and detection techniques, as well as wide-band, broadband, and ultra-wide-band CDMA systems for advanced wireless mobile communication systems. He has published more than 70 papers in journals and conference proceedings.

Dr. Yang received the Royal Society Sino-British Fellowship in 1997.

Lajos Hanzo (M'91–SM'92) received the degree in electronics in 1976 and the doctorate degree in 1983, both from the Technical University of Budapest, Hungary.

During his 26-year career in telecommunications, he has held various research and academic posts in Hungary, Germany, and the U.K. Since 1986, he has been with the Department of Electronics and Computer Science, University of Southampton, Southampton, U.K., where he holds the Chair in Telecommunications. He has coauthored eight books on mobile radio communications, published about 400 research papers, organized and chaired conference sessions, presented overview lectures, and been awarded a number of distinctions. Currently, he is managing an academic research team working on a range of research projects in the field of wireless multimedia communications sponsored by industry, the Engineering and Physical Sciences Research Council (EPSRC) U.K., the European IST Programme, and the Mobile Virtual Centre of Excellence, U.K. He is an enthusiastic supporter of industrial and academic liaison and offers a range of industrial courses.

Prof. Hanzo is an IEEE Distinguished Lecturer.